

Shapefinders: a new shape diagnostic for large scale structure.

Varun Sahni^a, B.S. Sathyaprakash^b, Sergei F. Shandarin^c

^aInter-University Centre for Astronomy & Astrophysics, Post Bag 4, Pune 411007, India

^bDepartment of Physics and Astronomy, UWCC, Cardiff, CF2 3YB, U.K.

^cDepartment of Physics and Astronomy, University of Kansas, Lawrence, KS 66045

ABSTRACT

We construct a set of shape-finders which determine shapes of compact surfaces (isodensity surfaces in galaxy surveys or N-body simulations) without fitting them to ellipsoidal configurations as done earlier. The new indicators arise from simple, geometrical considerations and are derived from fundamental properties of a surface such as its volume, surface area, integrated mean curvature and connectivity characterized by the Genus. These ‘Shapefinders’ could be used to diagnose the presence of filaments, pancakes and ribbons in large scale structure. Their lower-dimensional generalization may be useful for the study of two-dimensional distributions such as temperature maps of the Cosmic Microwave Background.

Subject headings: Cosmology—galaxies: clustering—large scale structure of the universe—methods: analytical, numerical .

The large scale structure of the Universe is remarkably rich in visual texture. At different density thresholds the clustering pattern has been variously described as ‘meatball-like’, ‘sponge-like’, ‘bubble-like’, ‘network of surfaces’ etc. (Zeldovich, Einasto & Shandarin 1982, Melott 1990, de Lapparent, Geller, & Huchra 1991). Attempts to quantify this pattern, in red-shift surveys of galaxies and in N-body simulations, have been made using topological discriminators such as the genus curve and percolation statistics (Zeldovich 1982, Shandarin 1983, Gott, Melott, & Dickinson 1986; for a recent discussion see Sahni, Sathyaprakash & Shandarin 1997), and also by applying minimal spanning trees and statistics sensitive to ‘shape’ (Babul & Starkman 1992, Luo & Vishniac 1995, Sathyaprakash, Sahni & Shandarin 1996a, Davé et al. 1997, for a review see Sahni & Coles 1995).

Recently Minkowski functionals have been used to characterize the *global* geometrical and topological properties of pointwise distributions, e.g. galaxy or cluster catalogues (Mecke et al. 1994). In this paper we suggest to use a set of geometrical parameters derived from Minkowski functionals to describe the geometry and topology of *individual* objects such as superclusters of galaxies. Minkowski functionals have a very convenient property of additivity and therefore they can be used for both an isolated structure (such as a cluster or supercluster of galaxies) or for a group of structures (such as all structures in an N-body simulation or a galaxy catalog). Probably using the Minkowski functionals themselves is the most general and universal approach to quantitatively representing the geometry of superclusters and voids, but often we are interested in the characteristic dimensions of an object as well. We have therefore devised *Shapefinders* – statistics having dimensions of [Length] as well as dimensionless statistics to characterize the morphology of large scale structure.

The morphology of superclusters and voids is likely to differ for different scenarios of structure formation and a study of supercluster-void shapes could help distinguish between radically different alternatives such as gravitational instability, seed models of structure formation and models based on explosions or ‘mini-bangs’.

It is well known that systems evolving under gravitational instability percolate at higher density thresholds corresponding to progressively lower values of the filling factor, which suggests that structures in the percolating phase are more likely to be sheet- or filament-like since sheets and filaments occupy a larger surface area than a sphere at a given volume, and therefore percolate more easily (Klypin & Shandarin 1993, Sathyaprakash, Sahni & Shandarin 1996a) For a fluid that has evolved as a result of gravitational instability, a low filling factor at percolation is also suggested by the Zeldovich approximation which predicts that the first singularities to form are pancake-like (Zeldovich 1982, Shandarin & Zeldovich 1989). However, it is unlikely that these pancakes will be strictly planar objects. Instead it is more natural that they will resemble, in a manner of speaking, the curved two-dimensional surface of a cup (Arnol'd, Shandarin, & Zeldovich 1982, Shandarin et al. 1995). Recent work suggests that soon after pancake formation, the density distribution becomes dominated by filaments which act as bridges connecting neighboring clusters (Bond, Kofman & Pogosyan 1996, Sathyaprakash, Sahni & Shandarin 1996a), with pancakes remaining statistically significant¹.

Most galaxy catalogues reveal structures with typical scales ~ 50 Mpc., some such as the Great Wall, appear to be even bigger. The present finite size of surveys, together with the fact that most of them are limited to surveying galaxies within a wedge shaped region, prevents us from establishing whether the visual structures we see are truly filamentary (one-dimensional) or they appear filamentary because the geometry of the survey prevents us from acquiring a fully three-dimensional perspective (filaments in a wedge type survey could, for instance, be slices of two-dimensional ‘sheets’). Upcoming large red-shift surveys such as the 2dF survey at the Anglo-Australian Telescope and the Sloan Digital Sky Survey promise to reveal large scale structures in their full glory and shed more light on their three-dimensional shapes.

The importance of trying to quantify shapes of clusters and superclusters, in galaxy surveys and in simulations has, in recent years, led to a discussion of different statistical tools which may be sensitive to ‘shape’. While such statistics have had a measured amount of success, it is fair to say that none of them is entirely satisfactory. A central feature of some shape indicators is that they describe the shape of a collection of points (equivalently – an overdense region) by evaluating its moment of inertia tensor, which is similar to fitting by an ellipsoid. The ratios of the principal axes then provide a means of ascertaining whether the structure is oblate or prolate. This method has been widely used in determining the luminosity profiles of galaxies and remains a powerful tool for classifying the projected shapes of ellipticals. Its efficacy as a discriminator for large scale structure is, however, not quite as obvious. Whereas general physical principles suggest that the shapes of galaxies should be predominantly elliptical or spiral, the shape of overdense regions in large scale structure (clusters and superclusters of galaxies) is likely to be far more complicated and less prone to a classification in terms of ‘eikonal’ shapes such as ellipsoids. Indeed, results of N-body simulations show that, when viewed at different density thresholds, shapes of compact surfaces can vary widely, ranging from approximately ellipsoidal (at high densities), to topologically complicated ‘spongy’ shapes at moderate density thresholds.

An example of a multiply-connected surface often seen at moderate thresholds in simulations is a

¹It is worth stressing the difference between formation of pancakes, filaments, or clumps and topological properties of density fields. According to the definition of Zeldovich, pancakes form in regions of three stream-flows or between shock fronts. Other authors however label any flattened region as a pancake. In any *generic* density field regions having densities above a sufficiently high thresholds look like compact regions (all three dimensions are similar). At a lower threshold ρ_1 the connected structure forms in the higher density regions $\rho > \rho_1$, the lower density regions $\rho < \rho_1$ remain connected (in other words both percolate). Then, at even lower threshold $\rho_2 < \rho_1$ the lower density regions $\rho < \rho_2$ cease percolating. The second percolation transition is sometimes associated with the formation of pancakes (e.g. Bond, Kofman & Pogosyan 1996).

torus. Clearly a statistic which attempts to describe the shape of a torus by fitting with an ellipsoid would be widely off the mark since it would lead us to conclude that the torus has a pronounced oblate shape and would miss completely its tubular form – which is more like a one-dimensional filament. A tendency to model shapes using pre-defined ‘eikonal’ forms, can lead to an exaggerated emphasis of oblateness or sphericity over filamentarity and could easily bias our understanding of the morphology of large scale structure (Sathyaprakash, Sahni, Shandarin & Fisher 1997). In this paper we introduce new ‘shape finders’ which are free from the above drawbacks, and probe the shape of an object without any preordained reference to an eikonal shape.

A compact surface, which could be an isodensity contour above or below a given density threshold in an N-body simulation, can be characterized by the following four quantities²: (i) Volume V , (ii) surface area S , (iii) integrated mean curvature: $C = \frac{1}{2} \int (\kappa_1 + \kappa_2) dS$, (iv) integrated Gaussian curvature (genus): $\mathcal{G} = -\frac{1}{4\pi} \int \kappa_1 \kappa_2 dS$, where $\kappa_1 \equiv 1/R_1$ and $\kappa_2 \equiv 1/R_2$ are the principal curvatures of the surface. Multiply-connected surfaces have $\mathcal{G} \geq 0$ while simply connected have $\mathcal{G} < 0$.

We introduce three *Shapefinders* each having dimensions of [Length]: $\mathcal{H}_i, i = 1, 2, 3$ where $\mathcal{H}_1 = V/S$, $\mathcal{H}_2 = S/C$ and $\mathcal{H}_3 = C$ (for multiply-connected surfaces C/\mathcal{G} may be more appropriate than C). Taken together, the trio \mathcal{H}_i provide robust and convenient measures of ‘shape’ as will be shown below. Based on \mathcal{H} we can also define a pair of very useful dimensionless Shapefinders: $\mathcal{K} \equiv (\mathcal{K}_1, \mathcal{K}_2)$ where

$$\mathcal{K}_1 = \frac{\mathcal{H}_2 - \mathcal{H}_1}{\mathcal{H}_2 + \mathcal{H}_1}, \quad \mathcal{K}_2 = \frac{\mathcal{H}_3 - \mathcal{H}_2}{\mathcal{H}_3 + \mathcal{H}_2}. \quad (1)$$

We note that $\mathcal{K}_{1,2} \leq 1$ by construction. \mathcal{K} can be regarded as a two-dimensional vector whose amplitude and direction determine the shape of an arbitrary three-dimensional surface. Combined with the genus, we get the dimensionless triad $(\mathcal{K}_1, \mathcal{K}_2, \mathcal{G})$ giving information about shape as well as topology. The Shapefinders \mathcal{H}_i , having dimensions of *length*, can be thought of as describing the spatial dimensions of an object. Thus, an ideal pancake (having vanishing thickness but not necessarily planar) has one characteristic dimension much smaller than the remaining two, so that $\mathcal{H}_1 \ll \mathcal{H}_2 \simeq \mathcal{H}_3$ and $\mathcal{K} \simeq (1, 0)$. An ideal filament (a one-dimensional object but not necessarily straight) has two characteristic dimensions much smaller than the third so that $\mathcal{H}_1 \simeq \mathcal{H}_2 \ll \mathcal{H}_3$ and $\mathcal{K} \simeq (0, 1)$. All three dimensions of a sphere are equal resulting in $\mathcal{H}_1 \simeq \mathcal{H}_2 \simeq \mathcal{H}_3$ and $\mathcal{K} \simeq (0, 0)$. In addition, an interesting surface to consider is a ‘ribbon’, for which $\mathcal{H}_1 \ll \mathcal{H}_2 \ll \mathcal{H}_3$ and $\mathcal{K} \simeq (1, 1)$.

The genus \mathcal{G} , integrated mean curvature C , and surface area S , can be derived for an arbitrary surface by considering its first and second fundamental forms. Consider a local coordinate patch on a surface of class $\geq C^2$, $\mathbf{r} \equiv \mathbf{r}(\theta, \phi)$, then the *first* (**I**) and *second* (**II**) fundamental forms of the surface are:

$$\begin{aligned} \mathbf{I} &= d\mathbf{r} \cdot d\mathbf{r} = E d\theta^2 + 2F d\theta d\phi + G d\phi^2 \\ \mathbf{II} &= -d\mathbf{r} \cdot d\mathbf{n} = L d\theta^2 + 2M d\theta d\phi + N d\phi^2 \end{aligned} \quad (2)$$

where \mathbf{n} is the unit normal to the surface $\mathbf{n} = \mathbf{r}_\phi \times \mathbf{r}_\theta / |\mathbf{r}_\phi \times \mathbf{r}_\theta|$, and

$$\begin{aligned} E &= \mathbf{r}_\theta \cdot \mathbf{r}_\theta, \quad G = \mathbf{r}_\phi \cdot \mathbf{r}_\phi, \quad F = \mathbf{r}_\phi \cdot \mathbf{r}_\theta \\ L &= \mathbf{r}_{\theta\theta} \cdot \mathbf{n}, \quad N = \mathbf{r}_{\phi\phi} \cdot \mathbf{n}, \quad M = \mathbf{r}_{\phi\theta} \cdot \mathbf{n}, \end{aligned} \quad (3)$$

$\mathbf{r}_\phi \equiv \partial\mathbf{r}/\partial\phi$, $\mathbf{r}_{\phi\phi} \equiv \partial^2\mathbf{r}/\partial\phi^2$, etc. As a result one gets (see e.g. Lipschutz 1969)

$$S = \int \int \sqrt{EG - F^2} d\phi d\theta$$

²These are also known as Minkowski functionals and have been applied to Cosmology by Mecke et al. 1994.

$$\begin{aligned}
\kappa_1 + \kappa_2 &= \frac{EN + GL - 2FM}{EG - F^2}, \\
\kappa_1 \kappa_2 &= \frac{LN - M^2}{EG - F^2} \\
C &= \int \int \frac{\kappa_1 + \kappa_2}{2} dS, \\
\mathcal{G} &= -\frac{1}{4\pi} \int \int \kappa_1 \kappa_2 dS.
\end{aligned} \tag{4}$$

We elaborate on the shape statistics by applying them to two surfaces – an ellipsoid and a torus. Consider first the triaxial ellipsoid having volume $V = \frac{4\pi}{3}abc$ and parametric form

$$\mathbf{r} = a(\sin \theta \cos \phi)\hat{x} + b(\sin \theta \sin \phi)\hat{y} + c(\cos \theta)\hat{z} \tag{5}$$

where $0 \leq \phi \leq 2\pi$, $0 \leq \theta \leq \pi$.

Results for the trio of dimensionful Shapefinders $\mathcal{H}_i \equiv (V/S, S/C, C)$ and the dimensionless Shapefinders $\mathcal{K} \equiv (\mathcal{K}_1, \mathcal{K}_2)$ are shown in Tables 1 & 2 for the triaxial ellipsoid with axis (a, b, c) and its deformations into a pancake, filament and sphere respectively. In all cases the Shapefinders have been normalized to give $\mathcal{H}_i = R$ ($\mathcal{K}_i = 0$) for a sphere of radius R .

Our results for idealized ‘eikonal’ surfaces are as follows: pancakes $(a, b = a, c)$, $a \gg c$, $\mathcal{K} \simeq (1, 0)$; filaments $(a, b, c = b)$, $a \gg b$, $\mathcal{K} \simeq (0, 1)$; ribbons (a, b, c) , $a \gg b \gg c$, $\mathcal{K} \simeq (1, 1)$; spheres $(a, b = a, c = a)$, $\mathcal{K} \simeq (0, 0)$. Thus, the deformation of a sphere into a pancake or filament results in the accompanying increase in \mathcal{K} : $(0, 0) \rightarrow (1, 0)$ (pancake), or $(0, 0) \rightarrow (0, 1)$ (filament). While deforming a filament into a pancake (and vice versa) it is possible to encounter an intermediate surface which resembles a ribbon, for this surface $\mathcal{K} \simeq (\alpha, \alpha)$, $\alpha \leq 1$. Tables 1 & 2 also show an interesting symmetry between oblate and prolate ellipsoids. Consider an oblate ellipsoid (a, a, c) , with $\mathcal{K} = (\mathcal{K}_1, \mathcal{K}_2)$, then, for the prolate ellipsoid (a, c, c) , $\mathcal{K} = (\mathcal{K}_2, \mathcal{K}_1)$! For shapes close to spherical, both $\mathcal{K}_1, \mathcal{K}_2$ are small, and it is more appropriate to study the ratio $\mathcal{K}_i/\mathcal{K}_j$ to assess departure from sphericity. Thus for pancakes $\mathcal{K}_1/\mathcal{K}_2 > 1$, filaments $\mathcal{K}_2/\mathcal{K}_1 > 1$ and for ribbons $\mathcal{K}_1/\mathcal{K}_2 \simeq 1$. In addition the statistic $\mathcal{K}_{1,2}^p$, $p < 1$, will also accentuate small departures from sphericity.

Next we consider a torus with elliptical cross-section having the parametric form

$$\mathbf{r} = (b + c \sin \phi) \cos \theta \hat{x} + (b + c \sin \phi) \sin \theta \hat{y} + a(\cos \phi)\hat{z} \tag{6}$$

where $a, c < b$, $0 \leq \phi, \theta < 2\pi$. The toroidal tube with diameter $2\pi b$ has an elliptical cross-section, a & c being respectively radii of curvature perpendicular and parallel to the plane of the torus. The usual circular torus is given by $a = c$.

Table 3 shows \mathcal{K} & \mathcal{H} for a torus with an elliptical cross-section which is an interesting surface since, like the triaxial ellipsoid, it has three sets of numbers defining its shape but it also has a hole which makes it topologically non-trivial. Such surfaces (with holes) generically arise in large scale structure surveys and in N-body simulations, especially at moderate density thresholds. Our results for the torus are qualitatively similar to those for the ellipsoid but with interesting new features. For instance one has two possibilities for a ribbon: Ribbon1 resembles a finger-ring, whereas Ribbon2 is a disc-with-large-hole, see Fig.1. (In the extreme case $c \simeq b$, Ribbon2 becomes like Pancake2, and, for $a \simeq b$, Ribbon1 becomes like Pancake1.)

Finally, for both the ellipsoid and the torus, \mathcal{K} remains invariant under a similarity transformation: $(a, b, c) \rightarrow (\alpha a, \alpha b, \alpha c)$.

It is quite remarkable that \mathcal{H} and \mathcal{K} give compatible results for similar shapes obtained by deforming two very dissimilar bodies, a torus and an ellipsoid. We feel this indicates that the Shapefinders introduced by us are robust and can be used for identifying topologically complicated shapes. In a companion paper we shall apply the shape-statistic to N-body simulations (Shandarin, Sathyaprakash & Sahni 1997)³. As emphasised by Sathyaprakash, Sahni & Shandarin 1996a, shape diagnosis combined with percolation theory provide a powerful tool with which to study gravitational clustering. Percolation theory demonstrates that the number of clusters/voids in a simulation always peaks at a threshold just above/below percolation. Thus, it makes sense to study shapes of individual clusters/voids at this threshold since the number of distinct isolated surfaces (boundaries of clusters/voids) is largest. In addition, it is likely that most surfaces at such low thresholds will be multiply-connected with a large genus, perhaps making it appropriate to define the third shape statistic to be C/\mathcal{G} instead of C as we have been assuming so far.

The statistic suggested by us could also be used to study more general shapes than those appearing in large scale structure. For instance one could use them to study the shapes of concentrated cosmic magnetic fields which might have important astrophysical consequences (Ryu et al. 1997). Finally, the two-dimensional Shapefinders $\mathcal{H}_1 = S/L$, $\mathcal{H}_2 = L$ and $\mathcal{K} = (\mathcal{H}_2 - \mathcal{H}_1)/(\mathcal{H}_2 + \mathcal{H}_1)$ (L is the circumference of a curve bounding a two-dimensional area S), combined with the two-dimensional genus, could prove useful when studying shapes and topologies of two-dimensional contours defining ‘hot and cold spots’ in the Cosmic Microwave Background, or isodensity surfaces in projection data. (Values of \mathcal{K} range from zero for a circle to unity for a filament.)

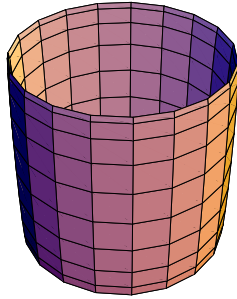
Acknowledgments: We acknowledge stimulating discussions with Sanjeev Dhurandhar and Somak Raychaudhury. SFS acknowledges financial support from the NSF-EPSCoR program and NASA grant NAG5-4039.

³It is interesting that other Shapefinders besides those mentioned above, can be constructed out of the four Minkowski functionals V, S, C and \mathcal{G} . For instance the dimensionless pair $\mathbf{\Delta} \equiv (\Delta_1, \Delta_2)$, where $\Delta_1 = S^3/V^2 - 1$, $\Delta_2 = (C^2/S)^3 - 1$, is also a good probe of pancakes, filaments and ribbons. $\mathbf{\Delta}$ shares many of the features of \mathcal{K} (the main difference being that, unlike \mathcal{K} , $\mathbf{\Delta}$ is not bounded from above $\Delta_{1,2} \geq 0$). If like \mathcal{K} , we normalise $\mathbf{\Delta}$ so that $\Delta_{1,2} = 0$ for spheres, then, for (i) pancakes $\Delta_1 > \Delta_2$, (ii) filaments $\Delta_2 > \Delta_1$, (iii) ribbons $\Delta_1 \simeq \Delta_2 \neq 0$.

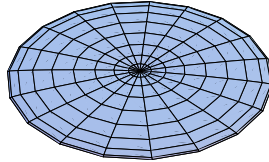
REFERENCES

- Arnol'd, B.I., Shandarin, S.F., & Zeldovich, Ya.B. 1982, *Geophys. Astrophys. Fluid Dynamics*, 20, 111
- Babul, A. and Starkman, G.D. 1992 *ApJ*, 401, 28.
- Klypin, A.A. & Shandarin, S.F. 1993, *ApJ*, 413, 48
- Bond, J.R., Kofman, L. & Pogosyan, D. 1996, *Nature*, 380, 603.
- Davé, D., Hellinger, D., Primack, J., Nolthenius, R. & Klypin, A., 1997, *MNRAS*, 284, 607
- de Lapparent, V., Geller, M.J. & Huchra, J.P. 1991, *ApJ*, 369, 273
- Gott, J.R., Melott, A.L. & Dickinson, M. 1986, *ApJ*, 306, 341
- Gott, J.R., Weinberg, D.H. & Melott, A.L., 1987, *ApJ*, 319, 1
- Lipschutz, M.M., 1969, *Theory and problems of Differential Geometry*, McGraw Hill.
- Luo, S. & Vishniac, E.T., 1995, *Astrophys. J. Suppl.* 96, 429.
- Mecke, K.R., Buchert, T. & Wagner, H., 1994, *Astron. Astrophys.*, 288, 697.
- Melott, A.L. 1990, *Physics Reports*, 193, 1
- Biermann, P. L., Kang, H., Rachen, J., & Ryu, D., 1997, in *Proc. of Moriond Meeting on High Energy Phenomena, Les Arcs*
- Sahni, V. & Coles, P., 1995, *Physics Reports*, 262, 1
- Sahni, V., Sathyaprakash, B.S. & Shandarin, S.F. 1997, *ApJ* 476, L1
- Sathyaprakash, B.S., Sahni, V. & Shandarin, S.F. 1996a, *ApJ*, 462, L5
- Sathyaprakash, B.S., Sahni, V., Shandarin, S.F. & Fisher, K. 1997, *MNRAS*, submitted
- Shandarin, S.F. 1983, *Soviet Astron. Lett.*, 9, 104
- Shandarin S.F., Melott, A.L., McDavitt, A., Pauls, J.L., & Tinker, J. 1995, *Phys. Rev. Lett.*, 75, 7
- Shandarin, S.F., Sathyaprakash, B.S. & Sahni, V. 1997, in preparation
- Shandarin, S.F. & Zeldovich Ya. B. 1989, *Rev. Mod. Phys.*, 61, 185
- Yess, C. & Shandarin, S.F. 1996, *ApJ*, 465, 2
- Zeldovich Ya. B. 1982, *Soviet Astron. Lett.*, 8, 102
- Zeldovich Ya. B., Einasto, J. & Shandarin, S.F. 1982, *Nature*, 300, 407

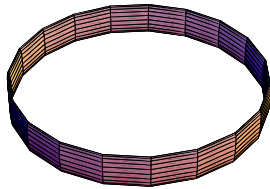
Pancake1



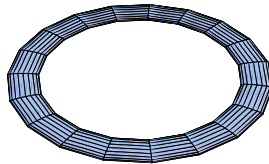
Pancake2



Ribbon1



Ribbon2



Filament



Sphere-with-hole

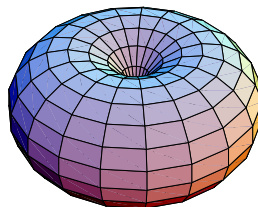


Fig. 1.— Deformations of a torus with an elliptical cross section.

Table 1: Shapefinders for a triaxial ellipsoid with axis a, b, c . ($V/S, S/C, C$ have dimensions of length, $\mathcal{K}_{1,2}$ are dimensionless.) The second column (M) is a description of the morphology of the object based on its dimensions: P= Pancake, F= Filament, R= Ribbon, S= Sphere.

a, b, c	M	$(\mathcal{K}_1, \mathcal{K}_2)$	V/S	S/C	C
(100, 100, 3)	P	(0.83, 0.10)	5.98	63.9	78.6
(100, 3, 3)	F	(0.10, 0.83)	3.82	4.70	50.2
(200, 20, 2)	R	(0.67, 0.67)	3.94	20.0	101
(100, 100, 100)	S	(0.99, 0.00)	100	100	100

Table 2: Deformations of a triaxial ellipsoid with axis a, b, c .

a, b, c	$(\mathcal{K}_1, \mathcal{K}_2)$
Sphere \rightarrow Filament	
(100, 100, 100)	(0.000, 0.000)
(100, 80, 80)	(0.004, 0.005)
(100, 50, 50)	(0.028, 0.054)
(100, 20, 20)	(0.077, 0.300)
(100, 10, 10)	(0.095, 0.540)
(100, 3, 3)	(0.100, 0.830)
Sphere \rightarrow Pancake	
(100, 100, 100)	(0.000, 0.000)
(100, 100, 80)	(0.005, 0.004)
(100, 100, 50)	(0.054, 0.028)
(100, 100, 20)	(0.300, 0.077)
(100, 100, 10)	(0.540, 0.095)
(100, 100, 3)	(0.830, 0.100)
Pancake \rightarrow Filament	
(100, 100, 3)	(0.830, 0.100)
(100, 70, 3)	(0.800, 0.130)
(100, 30, 3)	(0.650, 0.330)
(100, 10, 3)	(0.330, 0.650)
(100, 3, 3)	(0.100, 0.830)

Table 3: Shapefinders for a torus of radius b having an elliptical cross-section with axis a, c , ($b > a, c$). ($V/S, S/C, C$ have dimensions of length, $\mathcal{K}_{1,2}$ are dimensionless.) The second column (M) is a description of the morphology of the object based on its dimensions: P1,P2=Pancake, F=Filament, R1,R2=Ribbon, S=Sphere-with-hole.

b, a, c	M	$(\mathcal{K}_1, \mathcal{K}_2)$	V/S	S/C	C
(100, 99, 3)	P1	(0.90, 0.03)	7.05	136	144
(100, 3, 99)	P2	(0.88, 0.20)	7.05	114	173
(100, 3, 3)	F	(0.14, 0.93)	4.5	6.00	157
(150, 20, 2)	R1	(0.70, 0.80)	4.64	25.9	235
(150, 2, 20)	R2	(0.70, 0.80)	4.64	25.9	235
(20, 19, 19)	S	(0.14, -0.09)	28.5	38.0	31.4